



Early 7,8-Dihydroxyflavone Administration Ameliorates Synaptic and Behavioral Deficits in the Young FXS Animal Model by Acting on BDNF-TrkB Pathway

Yu-shan Chen^{1,2} · Si-ming Zhang^{1,2} · Wei Tan² · Qiong Zhu^{1,2} · Chao-xiong Yue^{1,2} · Peng Xiang^{1,2} · Jin-quan Li^{1,2} · Zhen Wei^{1,2} · Yan Zeng^{1,2}

Received: 21 September 2022 / Accepted: 30 December 2022 / Published online: 21 January 2023
© The Author(s), under exclusive licence to Springer Science+Business Media, LLC, part of Springer Nature 2023

Abstract

Fragile X syndrome (FXS) is the leading inherited form of intellectual disability and the most common cause of autism spectrum disorders. FXS patients exhibit severe syndromic features and behavioral alterations, including anxiety, hyperactivity, impulsivity, and aggression, in addition to cognitive impairment and seizures. At present, there are no effective treatments or cures for FXS. Previously, we have found the divergence of BDNF-TrkB signaling trajectories is associated with spine defects in early postnatal developmental stages of *Fmr1* KO mice. Here, young fragile X mice were intraperitoneal injection with 7,8-Dihydroxyflavone (7,8-DHF), a high affinity tropomyosin receptor kinase B (TrkB) agonist. 7,8-DHF ameliorated morphological abnormalities in dendritic spine and synaptic structure and rescued synaptic and hippocampus-dependent cognitive dysfunction. These observed improvements of 7,8-DHF involved decreased protein levels of BDNF, p-TrkB^{Y816}, p-PLC γ , and p-CaMKII in the hippocampus. In addition, 7,8-DHF intervention in primary hippocampal neurons increased p-TrkB^{Y816} and activated the PLC γ 1-CaMKII signaling pathway, leading to improvement of neuronal morphology. This study is the first to account for early life synaptic impairments, neuronal morphological, and cognitive delays in FXS in response to the abnormal BDNF-TrkB pathway. Present studies provide novel evidences about the effective early intervention in FXS mice at developmental stages and a strategy to produce powerful impacts on neural development, synaptic plasticity, and behaviors.

Keywords Fragile X syndrome · Brain-derived neurotrophic factor · Tyrosine kinase B receptor · 7,8-Dihydroxyflavone · Dendritic spine · Learning and memory

Introduction

Fragile X syndrome (FXS) is a prevalent, inherited neurodevelopmental disorder and is associated with learning disabilities, seizures, hyperactivity, and autistic behaviors [1]. In the vast majority of cases, FXS is caused by excessive

expansions of a noncoding CGG repeat in the fragile X mental retardation 1 (*Fmr1*) gene, with transcriptional silencing of *Fmr1* and a consequent reduction of *Fmr1*-encoded protein (FMRP) [2]. FMRP deficiency affects the translational regulation of multiple proteins involved in regulation of dendritic morphology, synaptic function, and behavioral phenotypes including cognitive deficits, anxiety, impaired social interactions, hyperactivity, and aggression [3, 4]. In light of the genetic disorder of neurodevelopment, behavioral and neuronal abnormalities in FXS are often thought to be closely associated with biological and molecular mechanisms involving synaptic development. Especially, proteins altered in FXS are implicated in signaling pathways that regulate dendritic spine development [5–8], leading abnormally long and thin dendritic spines in the brains of individuals with FXS and the *Fmr1* knockout (KO) mice [7, 9]. However, mechanistic insights into the molecular components of these abnormalities remained unclear.

Yu-shan Chen and Si-ming Zhang contributed equally to this work.

✉ Yan Zeng
zengyan68@wust.edu.cn

¹ Hubei Province Key Laboratory of Occupational Hazard Identification and Control, School of Medicine, Brain Science and Advanced Technology Institute, Wuhan University of Science and Technology, Wuhan 430065, China

² Geriatric Hospital Affiliated to Wuhan University of Science and Technology, Wuhan, China

Among various growth-promoting signals implicated in the regulation of neuronal morphogenesis and synapse formation, brain-derived neurotrophic factor (BDNF) is one of the strongest candidates to regulate the formation and maturation of dendritic spines in postnatal development [10, 11]. BDNF signaling is required for normal brain function in both the developing and mature nervous systems [12, 13]. Moreover, BDNF and its high-affinity receptor tropomyosin-related kinase B (TrkB) are essential in various processes associated with functional and structural synaptic plasticity, learning, and memory [13–15]. Although the importance of BDNF-TrkB for neuronal morphogenesis and synaptic plasticity is well established, its putative implication in FXS pathologies is less clear. Several studies indicate that BDNF protein production is altered in the brain of *Fmr1* KO mice and several FMRP functions are modulated by BDNF signaling [16–18]. Our previous study has shown that the changed expression profile of BDNF during early phases of neuronal development, and we found the correlation between BDNF-TrkB signaling and mature spines in young FXS mice [19]. In this sense, BDNF-TrkB pathway impairments during the pivotal developmental period may be the key mechanisms underlying abnormal dendritic spine morphogenesis and cognitive dysfunction in FXS.

Several previously published studies support that applying the intervention strategies in the early developmental stages is critical to ameliorate pathological phenotypes of neurodevelopmental disorders [20–22]. Early intervention strategies during critical developmental periods exhibit successful improvement in autism spectrum disorder (ASD) before major symptoms develop [20, 23–25]. For example, early inhibition of group I mGlu signaling at development stage, but not in adulthood, could rescue dendritic spine abnormalities in *Fmr1* KO mice [26]. Early postnatal low-dose valproic acid (VPA) treatment improves ASD-like behaviors associated with sustained rescue of repetitive behavior and social deficits in a *shank3ab* KO zebrafish model [25]. Administration with lovastatin during the early age of *Fmr1* KO rats corrected associative learning deficits and also has lasting beneficial effects [23]. Moreover, clinical studies have demonstrated early intervention of problem behavior marked beneficial effects in children with FXS and ASD [20, 27–30]. Hence, understanding the mechanism underlying the effectiveness of early intervention for FXS is warranted further examination.

The present study examined the effect of early intervention psychopharmacological administration with TrkB agonist 7,8-DHF on FXS mouse model at the critical developmental stages. We measured the alterations of morphological, behavior, biochemical, molecular, and physiological by 7,8-DHF administration. The results showed that early treatments with 7,8-DHF can rescue spatial and fear memory impairments and alleviate immature dendritic

spines, hippocampal synaptic structure, and plasticity impairment in *Fmr1* KO mice. These effects were associated with augmented BDNF levels and TrkB-PLC γ 1-CaMK II signals. In vitro experiments also showed that TrkB or PLC γ agonists promoted dendrite branching and lengthening in cultured hippocampus neurons. In all, this study supports the notion that early pharmacological interventions with 7,8-DHF ameliorated the behavioral and synaptic abnormalities of *Fmr1* KO mice at pivotal developmental stages by acting on the BDNF-TrkB pathway.

Materials and Methods

Animals

All procedures were approved by the Wuhan University of Science and Technology (WUST, Wuhan, China) ethics committee with the number IACUC-2017032. Wild-type (WT) mice (FVB.129P2-Pde6b + Tyrc-ch/AntJ, stock#4828) and *Fmr1* knockout (KO) mice (FVB.129P2-Pde6b + Tyrc-ch *Fmr1*tm1Cgr/J, stock# 4624) were purchased from Jackson Laboratory (Bar Harbor, USA). *Fmr1* KO and WT mice were maintained on a 12 h dark/light cycle at 21–23 °C and 40–60% humidity facility with free access to food and water at the animal center of WUST. Animals were 2-week-old at the beginning of the experimental manipulation. Mice were allocated arbitrarily into different groups, and the number of each group is indicated in figure legends.

Drug Treatments

7,8-DHF powder was obtained from Sigma Aldrich (St Louis, MO). The powder was dissolved into 100 mg/ml stock solution with 17% DMSO and then dissolved to a concentration of 1 mg/ml with sterile saline (vehicle) for intraperitoneal delivery [5, 31]. We used 50 μ l dilution every 10 g of body weight per day. *Fmr1* KO and WT control mice at P14 were administered 5 mg/kg 7,8-DHF [32] through intraperitoneal injections once daily for 16 consecutive days. To determine the appropriate dose, mice were weighted daily. Untreated groups received the same volume of vehicle with the same schedule. Animals were sacrificed and subjected to histological and biochemical analysis after the last administration. Behavioral tests were started at P60. Mice were subjected to a Morris water maze for 7 days and then fear condition test for 2 days. Behavioral testing was conducted during the light phase of the circadian cycle, between 9.30 a.m. and 6.30 p.m. For in vitro experiments, primary neurons were treated with 7,8-DHF (0.5 μ M, 1 μ M, or 5 μ M) at DIV 4 for 3 days [32]. The TrkB inhibitor K252a (50 nM or 100 nM) at DIV 6 for 24 h [32, 33] or PLC γ agonist m-3M3FBS (25 μ M) at DIV 5 for 3 h were used [34]. After treatment,

we analyzed neural complexity including dendritic length and branches using immunofluorescent confocal microscopy.

Primary Hippocampal Neuron Culture

Primary hippocampal neuronal cultures from neonatal mice (postnatal day 0–1) were prepared as previously described [35]. Briefly, euthanized the mouse and then gently removed the intact brain into dissection medium. The hippocampus was dissected and digested with D-Hanks (Gibco, USA) containing 0.25% trypsin (Gibco, USA) for 10 min and then dissociated by repeated trituration. Dissociated neurons were plated at a concentration of 15×10^4 cells/cm² on plates pre-coated with poly-L-lysine. After being incubated in a 37 °C incubator with 5% CO₂ for 4 h, neurons were covered by neurobasal medium with 2% B27 and 1% L-glutamine. Half of the old medium were replaced twice every week.

Immunocytochemistry and Confocal Imaging

Cells fixed with 4% paraformaldehyde were rinsed three times with 0.1 M PBS. Fixed cells were permeabilized and then blocked with 0.05% Triton X-100 containing 5% bovine serum albumin (BSA) at room temperature for 1 h. After being incubated with primary antibodies overnight, cells were washed with PBS for three times and then incubated with fluorescent secondary antibodies for 2 h. Slices were mounted and then covered with Mowiol and coverslips. Visual inspection and image acquisition were done using a FV1000 confocal-IX81 microscope (FluoView1000-IX81, Olympus, Tokyo, Japan). At least one entire neuron was presented on the field of vision. To quantify the total length of dendrite trees and number of dendrite branches, at least 50 neurons randomly selected from 5 independent cultures per condition were analyzed. Automated quantification of neurite length and branches was performed using ImageJ software. All measurements were performed in a blinded way.

Western Blotting

Hippocampal total extracts and cultured neurons from mice were lysed in RIPA lysis buffer (Thermo Fisher Scientific) to collect protein samples. Western blotting was performed as described previously [5]. Immunoblots were probed with the primary and secondary antibodies as shown in Table S1. The immunoreactive membranes were imaged using Western Blotting Luminol Reagent (Bio-Red, 1,705,060) and quantified by ImageJ.

Golgi-Cox Staining and Dendritic Spine Analysis

The procedure for Golgi staining was adapted from Cheng et al. previously [36]. Neurons were stained with Golgi

using the FD Rapid Golgi Staining Kit (FD Neurotechnology, Columbia, MD, USA). After the staining, we used an Olympus BX51WI Microscope to obtain bright-field images of pyramidal neurons in CA1 area of hippocampus and qualified the dendritic spines in 3–8 neurons/mice (5 segments/neuron) by NeuroLucida software 9.0 (MicroBright Field, Williston, USA). Spines were calculated in five segments per neuron, and more than 3–8 neurons per mouse were studied. Spine number and length were scored in 10 µm segments of secondary dendrite from each imaged neuron. Dendritic spines were classified based on morphology into four categories: mushroom (with a large bulbous head and a thin neck), stubby (short spines with a thick head and without a well-defined neck), thin (filopodia-like protrusions with small head), and branched spine (with more than one head) [19, 37]. The percentage of spines in each classification of the total spines was calculated. All measures were performed by individuals blinded to the genotype.

Transmission Electron Microscopy (TEM)

TEM experiments were conducted as the previous studies [19, 38]. Samples were immersed in 1% osmium tetroxide for 2 h and then dehydrated in graded ethanol and embedded in epoxy resin. The 90-nm thickness ultrathin sections cutting by Leica ultracut ultramicrotome were counterstained using uranyl acetate and lead citrate. Electron micrographs were taken by an electron microscope (Tecnai G2 20 TWIN, FEI, USA). Synapse was detected by a vesicle-filled pre-synaptic structure and postsynaptic density (PSD) in the target area. We quantified the synaptic density, PSD thickness, width of the synaptic cleft, and length of the synaptic active zone for at least 60–80 electron microscopic images per group.

Slice Electrophysiology

Slice preparation and electrophysiological recordings were the same as previously described [39, 40]. Vehicle or 7,8-DHF-treated mice were decapitated, and the brains were quickly removed and immersed in the ice-cold artificial cerebrospinal fluid (ACSF, in mM: 124 NaCl, 3 KCl, 1.25 KH₂PO₄, 26 NaHCO₃, 2 CaCl₂, 1 MgCl₂, and 10 glucose, pH = 7.4 ± 0.5), which continuously bubbled with 95% O₂ and 5% CO₂. Hippocampal slices (400 µm) were prepared by vibratome slicing and incubated in the recovery chamber (0.5 h at 34–36 °C and 1 h at room temperature). Then acute slices were transferred to a recording chamber that perfused with ACSF (34 °C) at 2 ml/min. Basal synaptic transmission (BST) was evaluated by increasing the stimulating intensity, and field excitatory postsynaptic potentials (fEPSPs) was measured using an input–output curve. On the basis of this curve, the stimulus was adjusted to elicit a fEPSP

with approximately half the maximum slope. A 64-channel multielectrode (MED64) system (Alpha MED Science, Tokyo, Japan) was used to record fEPSPs [41]. Long-term depression (LTD) was induced by low-frequency stimulation consisting of 900 pulses at 1 Hz [42–44].

Morris Water Maze Test

Morris water maze (MWM) is commonly used to assess spatial learning and memory [5]. A circular white tank (1.2 m diameter) was filled with 0.5 m water (22 ± 2 °C) and divided into four quadrants. A 10-cm diameter circular platform was placed in the middle of the third quadrant 2–4 cm beneath the water surface. Mice were trained for 5 consecutive days, and the probe trial was performed on day 6. During training, a mouse was randomly placed in one of the four quadrants and allowed for the mouse to find the hidden platform (60 s-cut-off). On day 6, the platform was removed and the probe trial was performed. Time spending in the target quadrant was measured. After the probe trial, swimming speed and latency to reach the visible platform were determined. All trials were recorded by the EthoVision automated tracking system (EthoVision, Noldus Information Technology, Netherlands).

Fear Conditioning Test

Fear conditioning paradigm was slightly modified and performed as previously described [5]. During the training phase, mice were allowed to adapt to the training chamber for 180 s and then were delivered with a tone [75 dB, 2500 Hz; conditioned stimulus (CS)] for 30 s and an immediate 2 s, 0.75 mA foot shock [unconditioned stimulus (US)]. Three training sessions were performed. Freezing behavior, defined as the complete absence of movement except for respiration, was measured, and the data were analyzed using the FreezeFrame software (Actimetrics, IL, USA). On day two, mice were returned to the fear conditioning chamber for 180 s with no tone or shock presented. Two hours later, cued fear memory was tested and mice were placed in the same chamber modified with decorations of various shapes and a novel floor. Freezing behavior 180 s before and after the presentation of the tone was measured.

Statistical Analysis

All data were expressed as the means \pm standard error of measurement (SEM). Data of all experiments were analyzed using Prism software (GraphPad 9.2). For the comparison between two groups, differences were analyzed with an unpaired two-tailed Student's *t*-test. One-way ANOVA and two-way ANOVA followed by Bonferroni's post hoc tests

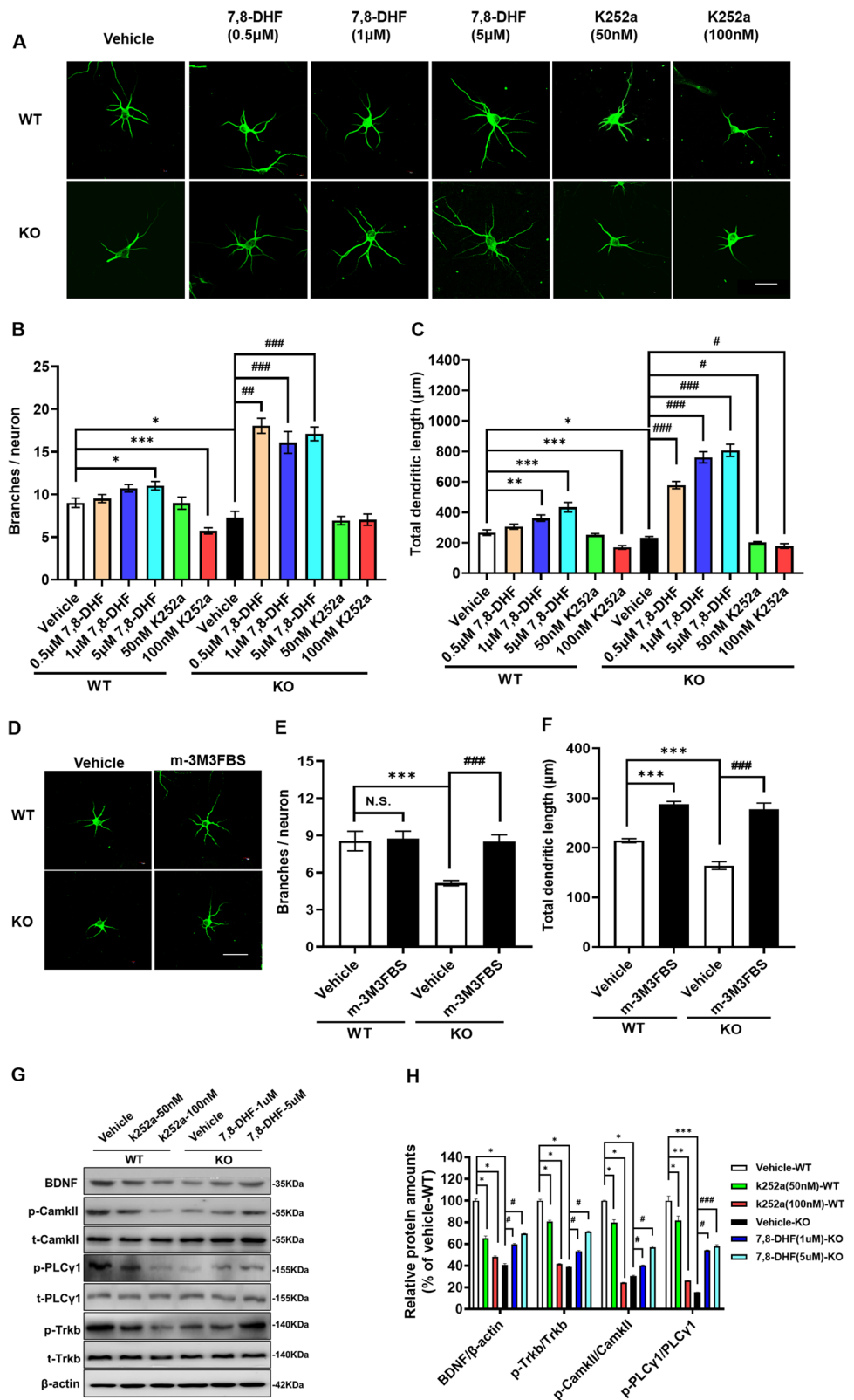
were used for multiple comparisons. Two-sided for *p* values < 0.05 were considered statistically significant.

Results

TrkB and PLC γ Agonists Improve Neuronal Morphology in Primary Neurons Obtained from *Fmr1* KO Mice

Since the activation of TrkB and PLC γ is downregulated and may cause the aberrant dendritic spines in *Fmr1* KO mice [19], we asked if TrkB and PLC γ agonists could improve hippocampal neuronal morphology in vitro. We therefore examined the dendritic length and branches in neurons treated with or without 7,8-DHF (TrkB agonist), m-3M3FBS (PLC γ agonist), or K252a (TrkB inhibitor). Firstly, we treated WT and KO primary neurons at 4 days in vitro (DIV 4) with 0.5, 1, or 5 μ M 7,8-DHF for 3 days. Additionally, to ensure that TrkB is required for dendritic morphogenesis, we used the TrkB inhibitor K252a (50 nM or 100 nM) at DIV 6 for 24 h. We observed that branches and total dendritic length were significantly decreased in KO cultures compared with that in WT cultures (branches: $df = 98, t = 2.145, p = 0.034$; length: $df = 98, t = 2.115, p = 0.037$). 7,8 DHF-treated (0.5 μ M) KO cultures exhibited a significant increase in numbers of branches and dendritic length compared to that in vehicle-KO group (branches: $df = 98, t = 9.777, p < 0.001$; length: $df = 98, t = 14.35, p < 0.001$). Whereas treated with 100 nM K252a, WT cultures showed decreased dendritic length and branches (branches: $df = 98, t = 4.951, p < 0.001$; length: $df = 98, t = 4.488, p < 0.001$) and KO cultures showed reduced dendritic length ($df = 98, t = 2.771, p < 0.05$) (Fig. 1A–C), which suggest the pivotal role of TrkB acting on neuronal maturation. To further examine the effect of TrkB downstream activation in neuronal maturation, we chose PLC γ , which is decreased in *Fmr1* KO mice. PLC γ agonist 25 μ M m-3M3FBS, when used at DIV 5 for 3 h, significantly increased the number of branches and dendritic length in vehicle-KO mice to levels that comparable to the vehicle-WT group (branches: $df = 98, t = 5.648, p < 0.001$; length: $df = 98, t = 7.604, p < 0.001$, Fig. 1D–F). Two-way ANOVA of branches and dendritic length showed a main effect of genotype [$F(1, 196) = 10.20, p = 0.002$; $F(1, 196) = 14.02, p < 0.001$], treatment [$F(1, 196) = 9.692, p = 0.002$; $F(1, 196) = 131.1, p < 0.001$], and genotype \times treatment interaction [$F(1, 196) = 7.522, p = 0.007$; $F(1, 196) = 5.829, p = 0.017$]. To further explore whether 7,8-DHF or K252a affects BDNF/TrkB-PLC γ 1-CaMK II signals which are downregulated in *Fmr1* KO mice, we monitored the expression of BDNF, TrkB, p-TrkB, PLC γ 1, p-PLC γ 1, CaMK II, and p-CaMK II in primary

Fig. 1 7,8-DHF improves hippocampal neuronal morphology caused by *Fmr1* deficiency in vitro. **A** Primary neurons were treated with 7,8-DHF (0.5 μ M, 1 μ M, or 5 μ M) at DIV 4 for 3 days or K252a (50 nM or 100 nM) at DIV 6 for 24 h. Representative images of DIV 7 cultures stained with MAP2. Scale bar = 30 μ m. Quantification of **B** dendritic branches and **C** total dendritic length in neuron cultures. **D** Primary neurons were treated with PLC γ agonist m-3M3FBS (25 μ M) at DIV 5 for 3 h and then staining with MAP2. Quantification of **E** dendritic branches and **F** total dendritic length in neuron cultures. *n* = 5 independent cultures per group \times 10 images per culture. **G, H** Western blot analysis of BDNF, phosphorylated and total TrkB, PLC- γ , and CaMKII (*n* = 3). Mean and SEM are shown. **p* < 0.05, ***p* < 0.01, and ****p* < 0.001 vs vehicle-WT; #*p* < 0.05, ##*p* < 0.01, and ###*p* < 0.001 vs vehicle-KO. N.S., not significant



neurons. Quantitative analysis revealed that 7,8-DHF treatment significantly elevated the levels of BDNF and p-TrkB and activated the downstream PLC γ 1-CaMK II signaling

pathways in KO cultures (Fig. 1G, H). As expected, K252a treatment decreased the BDNF/TrkB-PLC γ 1-CaMK II signals (Fig. 1G, H). Two-way ANOVA of BDNF, p-TrkB, p-PLC γ ,

and p-CaMKII levels showed a genotype \times treatment interaction [$F(2, 12) = 3251, p < 0.001; F(2, 12) = 9316, p < 0.001; F(2, 12) = 1533, p < 0.001; F(2, 12) = 5386, p < 0.0001$, respectively], a main effect of genotype [$F(1, 12) = 1229, p < 0.05; F(1, 12) = 5157, p < 0.05; F(1, 12) = 977.5, p < 0.05; F(1, 12) = 3816, p < 0.001$, respectively], and a main effect of treatment [$F(2, 12) = 267.2, p < 0.05; F(2, 12) = 852.7, p < 0.05; F(2, 12) = 308.3, p < 0.05; F(2, 12) = 1305, p < 0.001$, respectively]. Therefore, activation of TrkB-PLC γ pathway contributes to promote dendritic arborization and enhance neuronal maturation in *Fmr1* KO primary neurons.

TrkB Phosphorylation and Downstream PLC γ -CaMKII Signaling Pathway Are Normalized by TrkB Agonist 7,8-DHF in *Fmr1* KO Mice

Our previous study has suggested that BDNF/TrkB-PLC γ 1-CaMKII signaling is downregulated at the early stages of postnatal development in *Fmr1* KO mice [19]. To investigate whether aberrant TrkB and the downstream signaling pathways would be rescued by TrkB agonist 7,8-DHF, we first studied the activation status of p-TrkB, p-PLC γ , and p-CaMKII after treating P14 mice with 5 mg/kg 7,8-DHF daily for continuous 16 days (Fig. 2A). Quantitative analysis revealed higher protein levels of p-TrkB^{Y816} in 7,8-DHF-treated *Fmr1* KO mice than in vehicle-treated KO mice, whereas p-TrkB^{Y515} levels kept unchanged (Fig. 2A, B). Two-way ANOVA of p-TrkB^{Y816} levels showed a genotype \times treatment interaction [$F(1, 28) = 5.727, p = 0.024$], a main effect of genotype [$F(1, 28) = 4.410, p = 0.0449$], and a main effect of treatment [$F(1, 28) = 9.308, p = 0.005$]. In addition, levels of p-PLC γ and p-CaMKII were

significantly increased in 7,8-DHF-treated KO mice compared with vehicle-treated KO mice (Fig. 2A, C). Two-way ANOVA of p-PLC γ and p-CaMKII levels showed a genotype \times treatment interaction [$F(1, 28) = 9.578, p = 0.004; F(1, 28) = 4.646, p = 0.040$, respectively], a main effect of genotype [$F(1, 28) = 14.79, p < 0.001; F(1, 28) = 5.300, p = 0.029$, respectively], and a main effect of treatment [$F(1, 28) = 4.919, p = 0.035; F(1, 28) = 4.313, p = 0.047$, respectively]. Collectively, these results indicate that TrkB agonist 7,8-DHF rescued the deficient TrkB-PLC γ -CaMKII signaling in *Fmr1* KO mice.

Synaptic Loss and Synaptic Plasticity in *Fmr1* KO Mice Were Restored by TrkB Agonist 7,8-DHF

To test whether TrkB agonist 7,8-DHF also restores synaptic structure and function in *Fmr1* KO mice since it rescued deficient hippocampal TrkB-PLC γ -CaMKII signaling, we first examined spine density of pyramidal neurons in hippocampal CA1 using Golgi staining. Dendritic spines are the major sites for excitatory synaptic input and associated with synaptic development, maintenance, and plasticity [45]. Dendritic spines were classified into the following categories: mushroom, stubby, thin, and branched [37, 46]. Immature spines are long and thin, and mature spines become mushroom-like morphology. The morphology and turnover of spines are proxies for their maturity [47]. Neuropathological studies of FXS patients and in vivo imaging studies have both revealed the overabundance of immature dendritic spines in cortical pyramidal neurons, which contributes to the synaptic abnormality [47, 48]. In our study, vehicle-KO mice exhibited markedly increased thin, filopodia-like spines, and decreased mushroom spines compared with vehicle-WT mice, which was noticeably rescued by 7,8-DHF

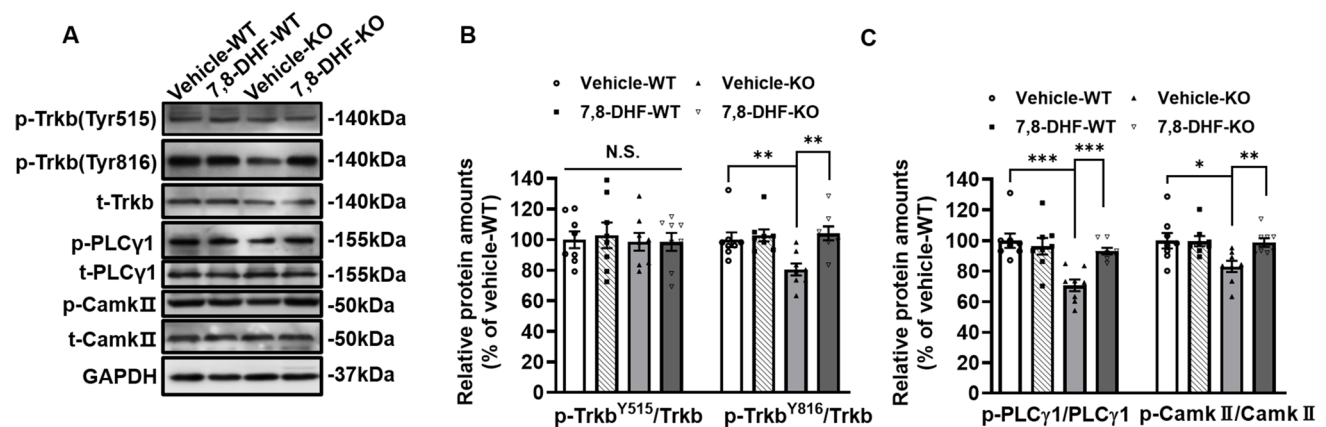


Fig. 2 Effects of 7,8-DHF intraperitoneal injection on BDNF downstream signaling in the hippocampus of WT and *Fmr1* KO mice. **A**, **D** Representative Western blots showing immunoreactivity for total and phosphorylated TrkB, PLC- γ , CaMKII. Data in **(B)** were nor-

malized to TrkB; data in **(C)** were normalized to PLC- γ and CaMKII, respectively; $n = 8$. Data are shown as mean \pm SEM. * $p < 0.05$, ** $p < 0.01$, and *** $p < 0.001$ vs vehicle-KO

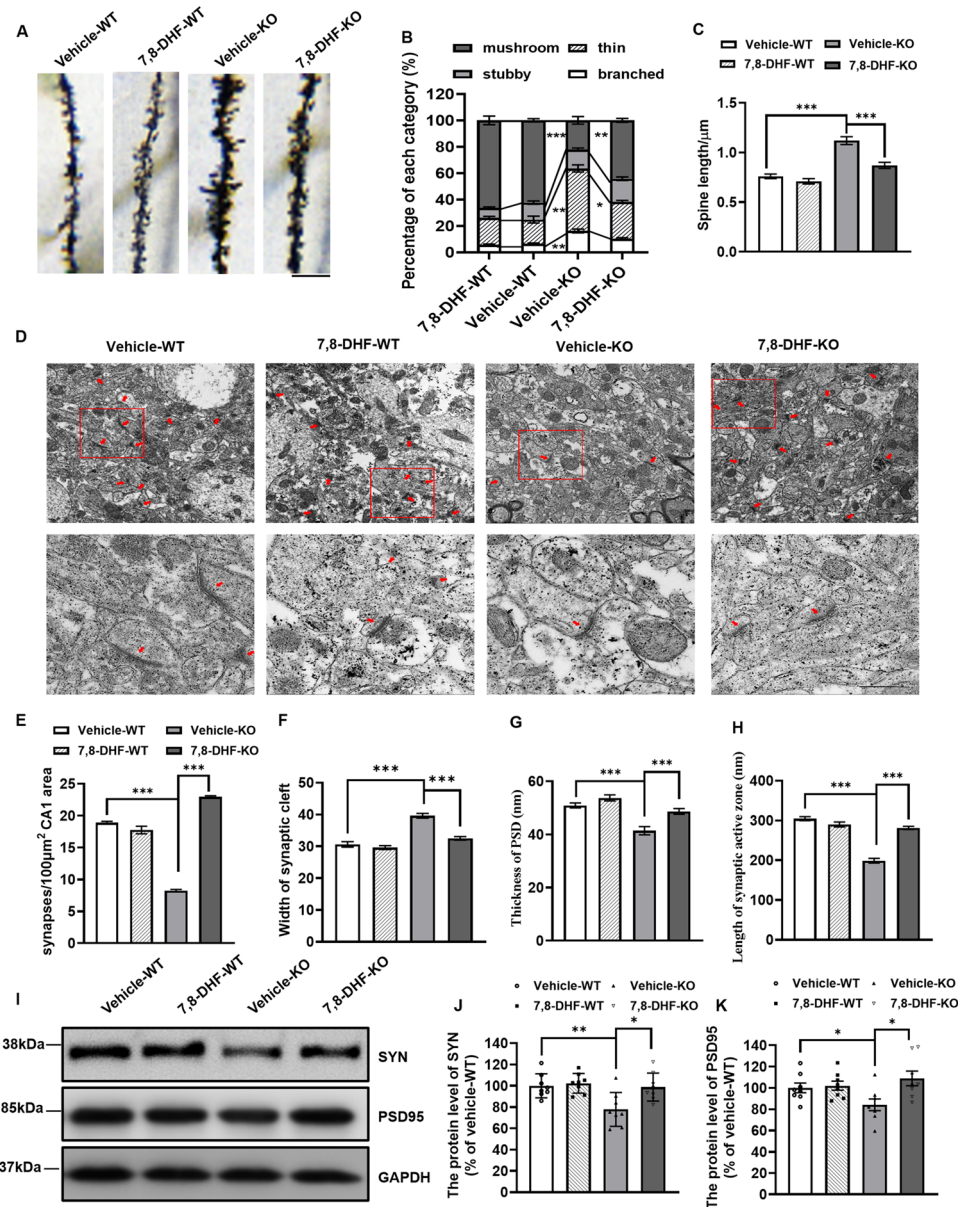


Fig. 3 Effects of 7,8-DHF intraperitoneal injection on dendritic spine density, synaptic structure, and protein levels of synaptophysin and PSD95 in the hippocampus CA1 of WT and *Fmr1* KO mice. **A** Photomicrograph of dendrites in CA1 pyramidal neurons of WT and *Fmr1* KO mice. Scale bar=5 μm. **B** Percentages of each category (mushroom, stubby, thin, and branched) of spines in pyramidal neurons per group. Error bars show SEM in all results. $n=5$ mice per group, 3–8 neurons per mouse, and 1 segment per neuron. $*p<0.05$, $**p<0.01$, and $***p<0.001$. **C** Quantification of spine length (spines per μm) on basal dendrites in the CA1 region. $n=5$ mice per group, 3–8 neurons per mouse, and 5 segments per neuron.

$***p<0.001$. **D** Representative electron microscopy schematic representation of CA1 area in hippocampus. Bar chart showing **E** density of synapses, **F** width of the synaptic cleft, **G** thickness of postsynaptic density (PSD), and **H** length of the synaptic active zone (scale bar: 1 or 0.5 μm). $n=5$ per group. Data presented mean±SEM. $***p<0.001$ vs vehicle-KO. **I** The protein levels of synaptophysin (SYN) and PSD95 detected by Western blot in the hippocampus. **J** SYN and **K** PSD95 levels were normalized to GAPDH and expressed as fold difference. $n=8$ mice per group. Values are mean±SEM. $*p<0.05$ and $**p<0.01$ vs vehicle-KO

treatment (Fig. 3A, B). Two-way ANOVA of thin and mushroom percentage showed a genotype×treatment interaction [$F(1, 16) = 28.48, p < 0.001$; $F(1, 16) = 16.64, p = 0.002$, respectively], a main effect of genotype [$F(1, 28) = 84.82, p < 0.001$; $F(1, 28) = 174.6, p < 0.001$,

respectively], and a main effect of treatment [$F(1, 28) = 18.56, p < 0.001$; $F(1, 28) = 30.68, p < 0.001$, respectively]. The numbers of stubby spines in CA1 regions were similar between vehicle-WT and vehicle-KO mice. The length of dendritic spines was significantly increased in

vehicle-KO mice compared to vehicle-WT mice but was remedied by 7,8-DHF treatment (Fig. 3A, C). Two-way ANOVA of spine length showed a genotype \times treatment interaction [$F(1, 16) = 10.70, p = 0.005$], a main effect of genotype [$F(1, 16) = 72.30, p < 0.001$], and a main effect of treatment [$F(1, 16) = 24.06, p < 0.001$].

We then utilized transmission electron microscopy (TEM) to compare the synaptic density and structure between groups in hippocampal CA1 of FXS mice (Fig. 3D). We found that Vehicle-KO hippocampus have less synapse, thinner PSD, and shorter synaptic active zone (Fig. 3D, E, G, H) but wider synaptic cleft than vehicle-WT group (Fig. 3D and 3F). Notably, 7,8-DHF treatment was sufficient to revert the decrease of synaptic density, PSD thickness, and length of the synaptic active zone and also revert the increase of synaptic cleft width (Fig. 3D–H). Two-way ANOVA of synaptic density, PSD thickness, length of the synaptic active zone, and synaptic cleft width showed a genotype \times treatment interaction [$F(1,361) = 329.2, p < 0.001; F(1,361) = 3.38, p = 0.067; F(1,361) = 69.35; F(1,361) = 17.22, p < 0.001$, respectively], a main effect of genotype [$F(1,361) = 38.55, p < 0.001; F(1,361) = 37.05, p < 0.001; F(1,361) = 96.03, p < 0.001; F(1,361) = 65.53, p < 0.001$, respectively], and a main effect of treatment [$F(1,361) = 241.2, p < 0.001; F(1,361) = 17.66, p < 0.001; F(1,361) = 33.76, p < 0.001; F(1,361) = 30.36, p < 0.001$, respectively].

We next examined levels of synaptophysin (SYN, pre-synaptic markers) and postsynaptic density protein 95 (PSD95, postsynaptic markers) using Western blot. Results showed a significant reduction in SYN and PSD95 in vehicle-KO mice, which was normalized in 7,8-DHF-KO mice (Fig. 3I–K). Two-way ANOVA of SYN levels showed a genotype \times treatment interaction [$F(1, 28) = 4.354, p = 0.046$], a main effect of genotype [$F(1, 28) = 8.314, p = 0.008$], and

a main effect of treatment [$F(1, 28) = 6.858, p = 0.014$]. Two-way ANOVA of PSD95 levels showed a genotype \times treatment interaction [$F(1, 28) = 4.400, p = 0.045$], a main effect of treatment [$F(1, 28) = 6.173, p = 0.019$], and no main effect of genotype. In all, these results suggest that 7,8-DHF treatment recovered abnormal synaptic structure in the hippocampus of *Fmr1* KO mice.

Given its effect on synaptic structure, we next examined whether 7,8-DHF restored synaptic plasticity in *Fmr1* KO mice. We tested low-frequency stimulation (LFS)-induced long-term depression (LTD) in each mice group and observed significantly larger LTD in vehicle-KO than in vehicle-WT mice ($87.24 \pm 3.66\%$ of baseline vs $62.07 \pm 1.59\%$ of baseline, $df = 8, t = 6.308, p < 0.001$, Fig. 4A, B). 7,8-DHF reduced LTD magnitude in KO mice ($52.04 \pm 6.63\%$ of baseline, $df = 8, t = 4.649, p = 0.002$, compared to the vehicle group, Fig. 4, B) but did not affect LTD in WT mice ($55.12 \pm 6.56\%$ of baseline, $df = 8, t = 1.030, p = 0.333$). Thus, 7,8-DHF appeared to rescue the enhanced LTD in *Fmr1* KO mice with no significant impact on WT mice. No significant difference in hippocampal LTP was observed in WT and *Fmr1* KO mice (data not shown). Taken together, synaptic structure and synaptic plasticity in *Fmr1* KO mice were restored by BDNF mimic and TrkB agonist, 7,8-DHF, suggesting BDNF-TrkB dysregulation in *Fmr1* KO mice is the underlying mechanism of synaptic development.

Learning and Memory Deficits in *Fmr1* KO Mice Were Rescued by TrkB Agonist 7,8-DHF

We first investigated the rescue effect in hippocampus-dependent learning and memory of 7,8-DHF; Morris water maze (MWM) was tested on 2-month-old *Fmr1* KO mice. The learning phase lasted 5 days. Two-way ANOVA of escape latency showed a main effect of genotype [$F(1, 44) = 9.71, p = 0.003$], treatment [$F(1, 44) = 6.521, p = 0.014$], and genotype \times treatment interaction [$F(1, 44) = 5.512, p = 0.024$]. During the learning

Fig. 4 Effects of 7,8-DHF intraperitoneal injection on synaptic plasticity in the hippocampus. **A** Low-frequency stimulation-induced LTD was measured in CA1 in slices prepared from vehicle-WT, vehicle-KO, 7,8-DHF-WT, and 7,8-DHF-KO mice. The figure shows the time course of the mean field excitatory postsynaptic potential (fEPSP) slope. $n = 5$ slices/5 mice. **B** Induction ratios of LTD. Mean and SEM are shown. *** $p < 0.001$

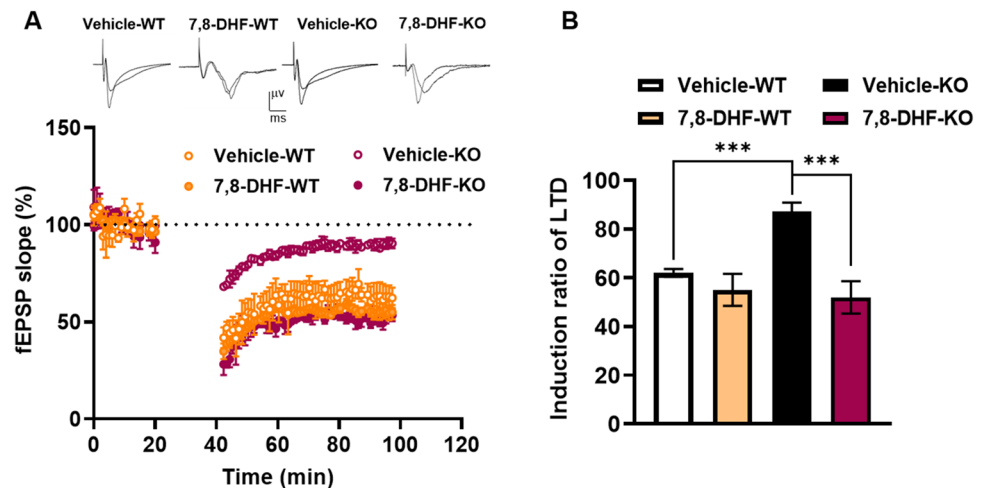
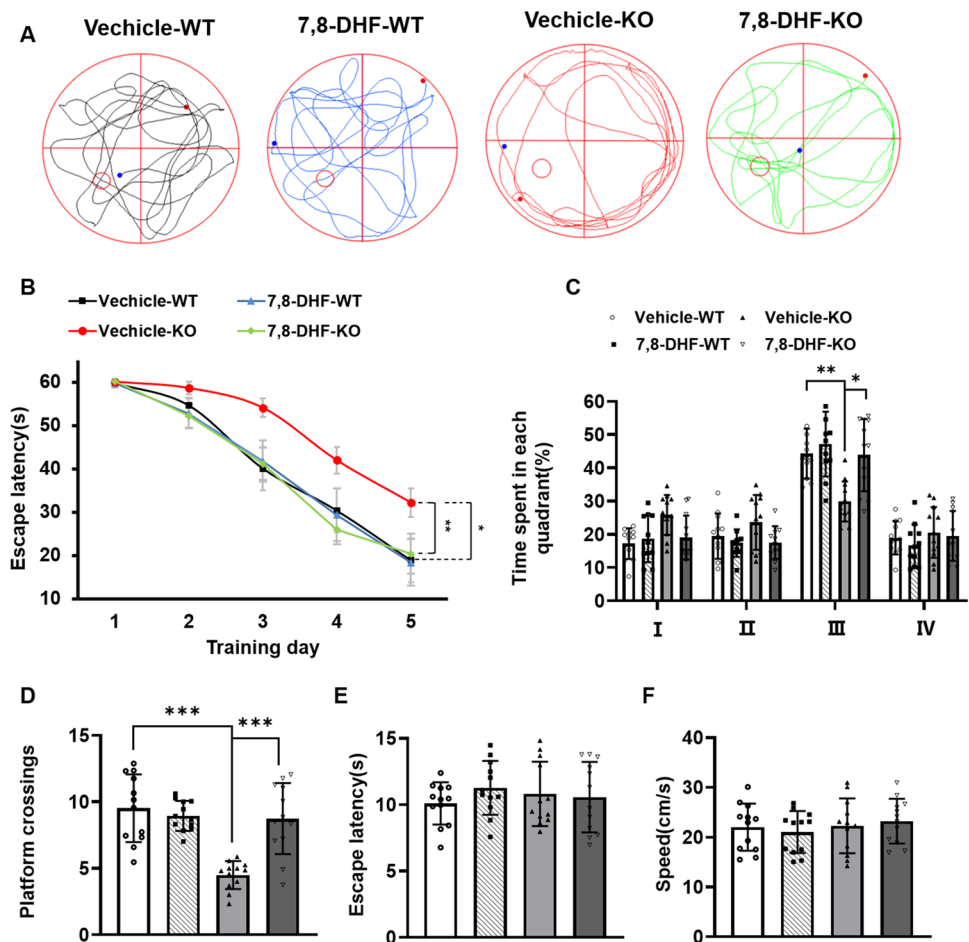


Fig. 5 Effect of 7,8-DHF intra-peritoneal injection on spatial learning and memory in *Fmr1* KO mice in the MWM test. **A** Representative track diagram of Morris water maze (MWM) test. **B** Means of escape latency from day 1 to day 5 of the training test (hidden platform trials). **C** Time spent in each quadrant during the probe trial test. The third quadrant is the region where the platform is located. **D** The number of platform crossings. There was no significant difference **E** in the latency and **F** in swimming speed among different animal groups. Error bars show SEM in all results. $n = 12$ mice per group. $**p < 0.01$ and $***p < 0.001$ vs vehicle-KO

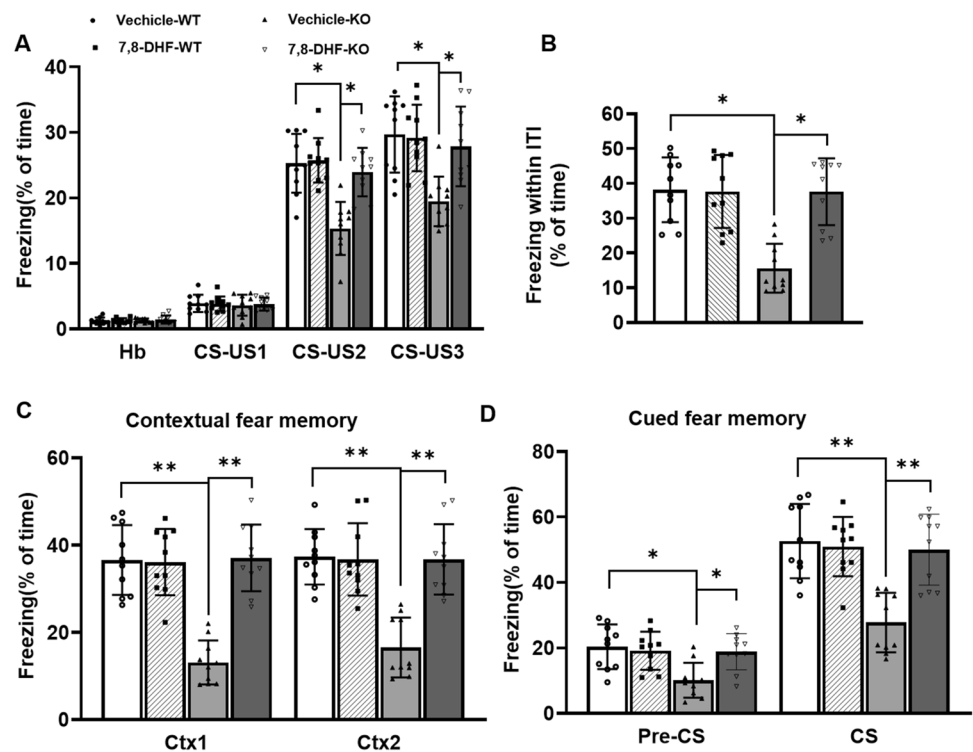


phase (Fig. 5A, B), *Fmr1* KO mice showed significantly longer escape latencies, which suggested impaired spatial memory acquisition. 7,8-DHF-KO mice located the hidden platform more quickly than vehicle-KO mice. In fact, 7, 8-DHF restored the performance of KO mice to the level of vehicle-WT mice (Fig. 5B). After 5 days of training sessions, the probe test was used to evaluate spatial memory by measuring the time spent in the correct quadrant after the removal of the hidden platform. Two-way ANOVA of time spending and platform crossings in the target quadrant showed a main effect of genotype [$F(1, 44) = 9.857, p = 0.003; F(1, 44) = 20.61, p < 0.001$], treatment [$F(1, 44) = 7.118, p = 0.011; F(1, 44) = 10.05, p = 0.003$], and genotype \times treatment interaction [$F(1, 44) = 5.932, p = 0.019; F(1, 44) = 17.45, p < 0.001$]. Vehicle-KO mice showed no preference for the correct quadrant and less platform crossings, whereas 7, 8-DHF-KO mice spent more time in the correct quadrant and crossed the previous location of the hidden platform as frequently as vehicle-WT mice did (Fig. 5C, D). In the visible-platform test, comparable motor and visual functions were observed among the four groups (Fig. 5E, F). Two-way ANOVA of escape latency and swimming speed showed no effect of genotype [$F(1, 44) = 0.0003$, not significant

(ns); $F(1, 44) = 0.80$, ns], treatment [$F(1, 44) = 0.528$, ns; $F(1, 44) = 0.0003$, ns], or genotype \times treatment interaction [$F(1, 44) = 1.236$, ns; $F(1, 44) = 0.515$, ns]. Therefore, variations in vision ability and swimming speeds did not cause behavioral differences among the groups.

We next tested whether 7,8-DHF normalizes the fear memory deficiencies in *Fmr1* KO mice. In fear conditioning test, 7,8-DHF showed a significant main effect of genotype [Hb: $F(1, 36) = 0.9259$, ns; CS-US1: $F(1, 36) = 0.182$, ns; CS-US2: $F(1, 36) = 22.37, p < 0.001$; CS-US3: $F(1, 36) = 11.94, p = 0.002$] and treatment [Hb: $F(1, 36) = 0.3707$, ns; CS-US1: $F(1, 36) = 0.021$, ns; CS-US2: $F(1, 36) = 13.23, p < 0.001$; CS-US3: $F(1, 36) = 5.581, p = 0.024$] as well as significant interactions [$F(1, 36) = 0.160$, ns; CS-US1: $F(1, 36) = 0.087$, ns; CS-US2: $F(1, 36) = 10.82, p = 0.002$; CS-US3: $F(1, 36) = 7.200, p = 0.011$] with fear acquisition in the training session. Freezing time in vehicle-KO mice was significantly lower compared to that in vehicle-WT mice during the second and third tone-shock pairs (Fig. 6A). During inter-trial intervals, vehicle-KO mice showed significantly less freezing time (Fig. 6B). Vehicle-KO mice also exhibited less freezing time when tested 24 h later for contextual fear and 48 h later for cued fear (Fig. 6C, D). In 7,8-DHF-KO mice, freezing time was

Fig. 6 Effect of 7,8-DHF intraperitoneal injection on fear memory in *Fmr1* KO mice. Mice were submitted to a training session and exposed to the context with or without receiving electrical foot shock. **A** Freezing time of mice from associative conditioned stimulus-unconditioned stimulus (CS-US) pairings. **B** Average freezing time during intertrial intervals (ITI). **C, D** Freezing time in contextual fear condition and in cued fear condition. Error bars show SEM. $n = 10$ mice per group. * $p < 0.05$ and ** $p < 0.01$ vs vehicle-KO



normalized in the training session (Fig. 6B), the contextual fear test (Fig. 6C), and the cued fear test (Fig. 6D).

Discussion

The present study was designed to test the effect of early therapeutic intervention on morphological and behavioral phenotypes in young FXS mice and to explore the underlying neural molecular mechanisms. Our results showed that early treatment of 7,8-DHF, a TrkB agonist, was capable of ameliorating neuronal morphology and function in *Fmr1* KO mice and successfully improved their memory performance (Fig. 7). The activating of BDNF-TrkB-PLC γ /CaMK II signaling pathway, as evidenced by the dramatic increases in phosphorylated TrkB (Tyr816), PLC γ , and CaMK II in hippocampus and primary cultured neurons, contributed to this pharmaceutical effect. These findings suggest that pharmaceutical treatment with TrkB agonist 7,8-DHF is an effective strategy for FXS and further provide the optimal window, the early developmental stages, for therapeutic intervention.

Evidence tends to support the view that early intervention for ASD must be implemented during developmentally critical period preferably before major symptoms such as social communication disorders develop [20, 49]. Research findings have also demonstrated that early psychopharmacological and environmental intervention improve cognitive impairment in young FXS individuals [28]. Early developmental stage is the key period for

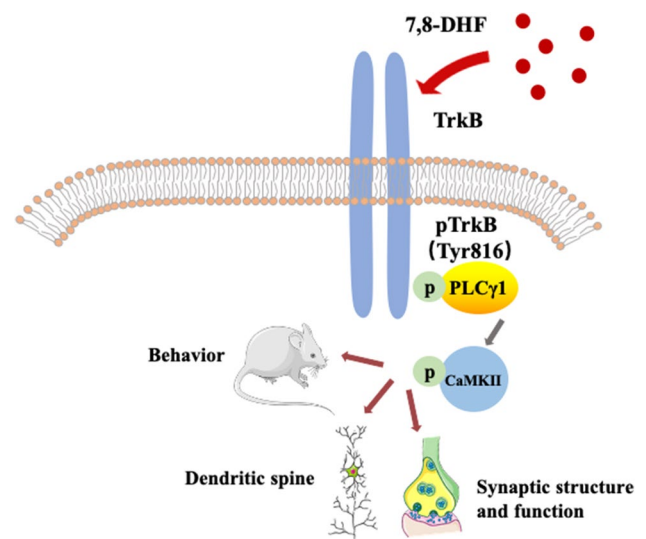


Fig. 7 Schematic illustration: 7,8-Dihydroxyflavone administration ameliorates synaptic structure and function, neuronal dendritic spine, and behavioral deficits in the young FXS mice by activating BDNF-TrkB-PLC- γ -CaMKII pathway

highly reorganized brain structure and function, formation of newborn neural circuits, and synaptic connections [24]. The treatment that miss this window may have limited effects. For example, early pharmacological intervention with mavoglurant exhibited more effective behavior improvement in the 0–3 days postfertilization in the zebrafish model of FXS; however, missing the optimal

time window has irreversible consequences [50]. Early treatment with lovastatin exhibited lasting correct alteration of associative learning deficits for at least 14 weeks in a FXS rat model, indicating the prevention of cognitive deficits and long-lasting benefits on cognition after early and transient therapeutic intervention [23]. In our study, FXS mice treated with 7,8-DHF starting at P14 showed long lasting improvements in the cognitive performances and synaptic function as still observed at about 4 weeks after treatment, indicating the therapeutic intervention at early postnatal ages is essential and effective. However, 7,8-DHF has different effects on different animal models. A recent study showed that a brief neonatal 7,8-DHF treatment is insufficient to produce long-lasting effects on behavior in the Ts65Dn mouse model of Down syndrome, indicating the timing of therapy with 7,8-DHF is a critical issue for attainment of positive effects on the brain [51].

Recently, treatments with 7,8-DHF rescued object location memory and normalized LTP in adult (3- to 5-month-old) *Fmr1* KO mice [52]. Our previous study also reported that activation of TrkB through chronic oral administration of 7,8-DHF is able to rescue dendritic spine phenotypes and attenuate behavioral abnormalities in *Fmr1* KO mice [5]. The present study further examined BDNF-TrkB signaling's role in early developmental period of *Fmr1* KO mice, i.e., P14-P30. In order to avoid the inestimable oral dose for unweaned mice at postnatal developmental stages, the mice received repeated intraperitoneal injections of 7,8-DHF for 16 consecutive days. Consistently, we found that TrkB activation by intraperitoneal injection of 7,8-DHF had beneficial effects on *Fmr1* KO mice but no effect on the WT mice, which suggests that at the appropriate dose of 7,8-DHF can treat FXS-specific pathological conditions. Intriguingly, in vitro application of 7,8-DHF in cultured hippocampal neurons also promoted neuronal dendritic development, suggesting the supporting role of 7,8-DHF on in vitro neuron development.

Previous studies have reported age-dependent alterations of BDNF protein levels that decreased in the hippocampus of *Fmr1* KO mice [53]. The levels of BDNF protein were reduced in the motor cortex and increased in the hippocampus of the adult *Fmr1* KO mice compared to WT mice [17]. However, no significant difference of BDNF expression was observed in the prefrontal cortex between *Fmr1* KO mice and WT control [17]. TrkB expression was significantly increased in an intermediate zone but reduced in the cortical plate of the embryonic neocortex in *Fmr1* KO mice, and no significant changes were found in the hippocampus, globus pallidus, and thalamic nuclei [17]. These data indicated differential expression profile of BDNF and region-specific spatial differences in BDNF and TrkB expression, which contributes to regional differences of synaptic plasticity in

Fmr1 KO mice. The absence of FMRP has been reported to result in an accumulation of BDNF mRNA [17]. The previous study investigated the effects of BDNF on expression of *Fmr1* mRNA and the effects of FMRP deficiency on BDNF and TrkB mRNA expression [18]. It was reported that BDNF treatment decreased *Fmr1* mRNA expression in cultured hippocampal neurons with increased TrkB protein expression and receptor phosphorylation [18]. This study also showed that TrkB downregulated *Fmr1* mRNA and protein levels. Moreover, TrkB, TrkC, and sortilin mRNAs are targets of FMRP [54, 55]. These studies suggest an interplay between BDNF/TrkB signaling and FMRP. However, the precise mechanism is currently unclear and requires further investigation in future study.

As known, BDNF-specific receptor TrkB is activated by autophosphorylation of its tyrosine residues, causing multiple intracellular signaling activation [14]. We therefore identified the specific signal pathway of 7,8-DHF acting by both in vivo and in vitro. We found that TrkB^{Y816} phosphorylation but not TrkB^{Y515} phosphorylation increased along with the induction of p-PLC γ and p-CaMKII after 7,8-DHF treatment, indicating that the TrkB-PLC γ -CaMKII pathway was responsible for the rescue by 7,8-DHF in *Fmr1* KO mice. These results are consistent with our previous report on the reduced activation of TrkB^{Y816} phosphorylation and PLC γ -CaMKII signaling and unchanged ERK pathway in *Fmr1* KO mice after treatment with 7,8-DHF or enriched environment [5, 19]. With TrkB^{Y515} phosphorylation, two main pathways occurred: the PI3K-AKT pathway and MAPK/ERK pathway, which activate antiapoptotic effects and protein translation respectively [56]. With TrkB^{Y816} phosphorylation, the PLC γ pathway is engaged, causing diacylglycerol production, increase in intracellular calcium, and the PKC and CAMK activation [57]. Seese et al. showed that 7,8-DHF increases synaptic TrkB phosphorylated at its Y515 site for activation of the ERK1/2 signaling pathway, in turn, may have effectors related to actin dynamics and learning [52]. Previous studies have demonstrated that systemic administration of 7,8-DHF significantly enhanced the activation of phosphorylated TrkB at the Y515 and Y816 sites as well as p-Erk1/2, p-CREB and p-CaMKII in 25-month-old SD rats and a rat model of schizophrenia, indicating that 7,8-DHF activates TrkB-ERK-CREB and TrkB-CaMKII-CREB signaling pathway in aging and schizophrenia models [58, 59]. Whereas in this study, TrkB^{Y816} phosphorylation was increased, through the activation of TrkB-PLC γ -CaMKII signaling pathway by 7,8-DHF treatment, we observed modulating changes in the spine dysmorphogenesis and abnormal synaptic function in *Fmr1* KO mice, and subsequently, an improvement in hippocampus-dependent learning and spatial and fear memory, as determined by MWM and conditional fear test.

In summary, we have been able to demonstrate that early intervention by TrkB stimulation with 7,8-DHF helps to establish and maintain the neural development and restore normal cognitive development in FXS. Further in-depth investigation of the understanding effective mechanisms for early intervention is warranted and will help develop future targeted treatments for FXS individuals.

Supplementary Information The online version contains supplementary material available at <https://doi.org/10.1007/s12035-023-03226-w>.

Acknowledgements We would like to thank Dr. Yuan Cao and Piao Zou at the Medicine & Sciences Analysis Center of Wuhan University of Science and Technology for the help on immunofluorescence analysis.

Author Contribution Yushan Chen and Yan Zeng conceived the idea, designed the project, and wrote the manuscript. Wei Tan contributed to revising the manuscript. Siming Zhang, Qiong Zhu, Chaoxiong Yue, and Peng Xiang performed the experiments and analyzed the data. Jinquan Li and Zhen Wei assisted with experiments and data analysis.

Funding This work was supported by grants from the Ministry of Science and Technology of China (2020YFC2006000) and the National Natural Science Foundation of China (NSFC, grant nos. 82071272, 81571095, and 81870901).

Data Availability The authors will provide the data under a reasonable request.

Declarations

Ethics Approval All procedures were approved by the Wuhan University of Science and Technology (WUST, Wuhan, China) ethics committee with the number IACUC-2017032.

Consent to Participate Not applicable.

Consent for Publication All authors read and approved the final manuscript.

Conflict of Interest The authors declare no competing interests.

References

- Hagerman RJ, Berry-Kravis E, Hazlett HC, Bailey DB Jr, Moine H, Kooy RF, Tassone F, Gantois I, et al (2017) Fragile X syndrome. *Nat Rev Dis Primers* 3:17065. <https://doi.org/10.1038/nrdp.2017.65>
- Hagerman RJ, Hagerman PJ (2022) Fragile X Syndrome: Lessons Learned and What New Treatment Avenues Are on the Horizon. *Annu Rev Pharmacol Toxicol* 62:365–381. <https://doi.org/10.1146/annurev-pharmtox-052120-090147>
- Richter JD, Zhao X (2021) The molecular biology of FMRP: new insights into fragile X syndrome. *Nat Rev Neurosci* 22(4):209–222. <https://doi.org/10.1038/s41583-021-00432-0>
- Wan RP, Zhou LT, Yang HX, Zhou YT, Ye SH, Zhao QH, Gao MM, Liao WP, et al (2017) Involvement of FMRP in Primary MicroRNA Processing via Enhancing Drosha Translation. *Mol Neurobiol* 54(4):2585–2594. <https://doi.org/10.1007/s12035-016-9855-9>
- Tian M, Zeng Y, Hu Y, Yuan X, Liu S, Li J, Lu P et al (2015) 7,8-Dihydroxyflavone induces synapse expression of AMPA GluA1 and ameliorates cognitive and spine abnormalities in a mouse model of fragile X syndrome. *Neuropharmacology* 89:43–53. <https://doi.org/10.1016/j.neuropharm.2014.09.006>
- Ferrante A, Boussadia Z, Borreca A, Mallozzi C, Pedini G, Pacini L, Pezzola A, Armida M et al (2021) Adenosine A(2A) receptor inhibition reduces synaptic and cognitive hippocampal alterations in Fmr1 KO mice. *Transl Psychiatry* 11(1):112. <https://doi.org/10.1038/s41398-021-01238-5>
- Pyronneau A, He Q, Hwang JY, Porch M, Contractor A, Zukin RS (2017) Aberrant Rac1-cofilin signaling mediates defects in dendritic spines, synaptic function, and sensory perception in fragile X syndrome. *Sci Signal* 10(504). <https://doi.org/10.1126/scisignal.aan0852>
- Gross C, Banerjee A, Tiwari D, Longo F, White AR, Allen AG, Schroeder-Carter LM, Krzeski JC et al (2019) Isoform-selective phosphoinositide 3-kinase inhibition ameliorates a broad range of fragile X syndrome-associated deficits in a mouse model. *Neuropharmacology* 44(2):324–333. <https://doi.org/10.1038/s41386-018-0150-5>
- He CX, Portera-Cailliau C (2013) The trouble with spines in fragile X syndrome: density, maturity and plasticity. *Neuroscience* 251:120–128. <https://doi.org/10.1016/j.neuroscience.2012.03.049>
- Chapleau CA, Larimore JL, Theibert A, Pozzo-Miller L (2009) Modulation of dendritic spine development and plasticity by BDNF and vesicular trafficking: fundamental roles in neurodevelopmental disorders associated with mental retardation and autism. *J Neurodev Disord* 1(3):185–196. <https://doi.org/10.1007/s11689-009-9027-6>
- Waterhouse EG, Xu B (2009) New insights into the role of brain-derived neurotrophic factor in synaptic plasticity. *Mol Cell Neurosci* 42(2):81–89. <https://doi.org/10.1016/j.mcn.2009.06.009>
- Almeida LE, Roby CD, Krueger BK (2014) Increased BDNF expression in fetal brain in the valproic acid model of autism. *Mol Cell Neurosci* 59:57–62. <https://doi.org/10.1016/j.mcn.2014.01.007>
- Zagrebelsky M, Korte M (2014) Form follows function: BDNF and its involvement in sculpting the function and structure of synapses. *Neuropharmacology* 76 Pt C:628–638. <https://doi.org/10.1016/j.neuropharm.2013.05.029>
- Gottmann K, Mittmann T, Lessmann V (2009) BDNF signaling in the formation, maturation and plasticity of glutamatergic and GABAergic synapses. *Exp Brain Res* 199(3–4):203–234. <https://doi.org/10.1007/s00221-009-1994-z>
- Luine V, Frankfurt M (2013) Interactions between estradiol, BDNF and dendritic spines in promoting memory. *Neuroscience* 239:34–45. <https://doi.org/10.1016/j.neuroscience.2012.10.019>
- Castrén ML, Castrén E (2014) BDNF in fragile X syndrome. *Neuropharmacology* 76 Pt C:729–736. <https://doi.org/10.1016/j.neuropharm.2013.05.018>
- Louhivuori V, Vicario A, Uutela M, Rantamäki T, Louhivuori LM, Castrén E, Tongiorgi E, Akerman KE et al (2011) BDNF and TrkB in neuronal differentiation of Fmr1-knockout mouse. *Neurobiol Dis* 41(2):469–480. <https://doi.org/10.1016/j.nbd.2010.10.018>
- Castrén M, Lampinen KE, Miettinen R, Koponen E, Sipola I, Bakker CE, Oostra BA, Castrén E (2002) BDNF regulates the expression of fragile X mental retardation protein mRNA in the hippocampus. *Neurobiol Dis* 11(1):221–229. <https://doi.org/10.1006/nbdi.2002.0544>
- Chen YS, Zhang SM, Yue CX, Xiang P, Li JQ, Wei Z, Xu L, Zeng Y (2022) Early environmental enrichment for autism spectrum disorder Fmr1 mice models has positive behavioral and molecular effects. *Exp Neurol* 114033. <https://doi.org/10.1016/j.expneurol.2022.114033>

20. Dawson G (2008) Early behavioral intervention, brain plasticity, and the prevention of autism spectrum disorder. *Dev Psychopathol* 20(3):775–803. <https://doi.org/10.1017/s0954579408000370>
21. Singer B, Friedman E, Seeman T, Fava GA, Ryff CD (2005) Protective environments and health status: cross-talk between human and animal studies. *Neurobiol Aging* 26(Suppl 1):113–118. <https://doi.org/10.1016/j.neurobiolaging.2005.08.020>
22. Meredith RM (2015) Sensitive and critical periods during neurotypical and aberrant neurodevelopment: a framework for neurodevelopmental disorders. *Neurosci Biobehav Rev* 50:180–188. <https://doi.org/10.1016/j.neubiorev.2014.12.001>
23. Asiminas A, Jackson AD, Louros SR, Till SM, Spano T, Dando O, Bear MF, Chattarji S, et al (2019) Sustained correction of associative learning deficits after brief, early treatment in a rat model of Fragile X Syndrome. *Sci Transl Med* 11(494). <https://doi.org/10.1126/scitranslmed.aao0498>
24. Sullivan K, Stone WL, Dawson G (2014) Potential neural mechanisms underlying the effectiveness of early intervention for children with autism spectrum disorder. *Res Dev Disabil* 35(11):2921–2932. <https://doi.org/10.1016/j.ridd.2014.07.027>
25. Liu C, Wang Y, Deng J, Lin J, Hu C, Li Q, Xu X (2021) Social Deficits and Repetitive Behaviors Are Improved by Early Postnatal Low-Dose VPA Intervention in a Novel shank3-Deficient Zebrafish Model. *Front Neurosci* 15:682054. <https://doi.org/10.3389/fnins.2021.682054>
26. Su T, Fan HX, Jiang T, Sun WW, Den WY, Gao MM, Chen SQ, Zhao QH et al (2011) Early continuous inhibition of group I mGlu signaling partially rescues dendritic spine abnormalities in the Fmr1 knockout mouse model for fragile X syndrome. *Psychopharmacology* 215(2):291–300. <https://doi.org/10.1007/s00213-010-2130-2>
27. Kurtz PF, Chin MD, Robinson AN, O'Connor JT, Hagopian LP (2015) Functional analysis and treatment of problem behavior exhibited by children with fragile X syndrome. *Res Dev Disabil* 43–44:150–166. <https://doi.org/10.1016/j.ridd.2015.06.010>
28. Winarni TI, Schneider A, Borodyanskara M, Hagerman RJ (2012) Early intervention combined with targeted treatment promotes cognitive and behavioral improvements in young children with fragile x syndrome. *Case Rep Genet* 2012:280813. <https://doi.org/10.1155/2012/280813>
29. Thurman AJ, Potter LA, Kim K, Tassone F, Banasik A, Potter SN, Bullard L, Nguyen V et al (2020) Controlled trial of lovastatin combined with an open-label treatment of a parent-implemented language intervention in youth with fragile X syndrome. *J Neurodev Disord* 12(1):12. <https://doi.org/10.1186/s11689-020-09315-4>
30. Reichow B, Hume K, Barton EE, Boyd BA (2018) Early intensive behavioral intervention (EIBI) for young children with autism spectrum disorders (ASD). *Cochrane Database Syst Rev* 5(5):Cd009260. <https://doi.org/10.1002/14651858.CD009260.pub3>
31. Wang J, Gao F, Cui S, Yang S, Gao F, Wang X, Zhu G (2022) Utility of 7,8-dihydroxyflavone in preventing astrocytic and synaptic deficits in the hippocampus elicited by PTSD. *Pharmacol Res* 176:106079. <https://doi.org/10.1016/j.phrs.2022.106079>
32. Zhang Z, Liu X, Schroeder JP, Chan CB, Song M, Yu SP, Weinschenker D, Ye K (2014) 7,8-Dihydroxyflavone prevents synaptic loss and memory deficits in a mouse model of Alzheimer's disease. *Neuropsychopharmacology* 39(3):638–650. <https://doi.org/10.1038/npp.2013.243>
33. Pei W, Meng F, Deng Q, Zhang B, Gu Y, Jiao B, Xu H, Tan J et al (2021) Electroacupuncture promotes the survival and synaptic plasticity of hippocampal neurons and improvement of sleep deprivation-induced spatial memory impairment. *CNS Neurosci Ther* 27(12):1472–1482. <https://doi.org/10.1111/cns.13722>
34. Bagayogo IP, Dreyfus CF (2009) Regulated release of BDNF by cortical oligodendrocytes is mediated through metabotropic glutamate receptors and the PLC pathway. *ASN Neuro* 1(1). <https://doi.org/10.1042/an20090006>
35. Beaudoin GM 3rd, Lee SH, Singh D, Yuan Y, Ng YG, Reichardt LF, Arikath J (2012) Culturing pyramidal neurons from the early postnatal mouse hippocampus and cortex. *Nat Protoc* 7(9):1741–1754. <https://doi.org/10.1038/nprot.2012.099>
36. Cheng K, Chen YS, Yue CX, Zhang SM, Pei YP, Cheng GR, Liu D, Xu L et al (2019) Calsyntenin-1 Negatively Regulates ICAM5 Accumulation in Postsynaptic Membrane and Influences Dendritic Spine Maturation in a Mouse Model of Fragile X Syndrome. *Front Neurosci* 13:1098. <https://doi.org/10.3389/fnins.2019.01098>
37. Bian WJ, Miao WY, He SJ, Qiu Z, Yu X (2015) Coordinated Spine Pruning and Maturation Mediated by Inter-Spine Competition for Cadherin/Catenin Complexes. *Cell* 162(4):808–822. <https://doi.org/10.1016/j.cell.2015.07.018>
38. Yue C, Li J, Jin H, Hua K, Zhou W, Wang Y, Cheng G, Liu D et al (2019) Autophagy Is a Defense Mechanism Inhibiting Invasion and Inflammation During High-Virulent Haemophilus parasuis Infection in PK-15 Cells. *Front Cell Infect Microbiol* 9:93. <https://doi.org/10.3389/fcimb.2019.00093>
39. Sanz-García A, Knafo S, Pereda-Pérez I, Esteban JA, Venero C, Armario A (2016) Administration of the TrkB receptor agonist 7,8-dihydroxyflavone prevents traumatic stress-induced spatial memory deficits and changes in synaptic plasticity. *Hippocampus* 26(9):1179–1188. <https://doi.org/10.1002/hipo.22599>
40. Pei YP, Wang YY, Liu D, Lei HY, Yang ZH, Zhang ZW, Han M, Cheng K et al (2020) ICAM5 as a Novel Target for Treating Cognitive Impairment in Fragile X Syndrome. *J Neurosci* 40(6):1355–1365. <https://doi.org/10.1523/jneurosci.2626-18.2019>
41. Huang CW, Hsieh YJ, Tsai JJ, Huang CC (2006) Effects of lamotrigine on field potentials, propagation, and long-term potentiation in rat prefrontal cortex in multi-electrode recording. *J Neurosci Res* 83(6):1141–1150. <https://doi.org/10.1002/jnr.20797>
42. Chatterjee M, Kurup PK, Lundbye CJ, Hugger Toft AK, Kwon J, Benedict J, Kamceva M, Banke TG et al (2018) STEP inhibition reverses behavioral, electrophysiologic, and synaptic abnormalities in Fmr1 KO mice. *Neuropharmacology* 128:43–53. <https://doi.org/10.1016/j.neuropharm.2017.09.026>
43. Arias-Cavieres A, Barrientos GC, Sánchez G, Elgueta C, Muñoz P, Hidalgo C (2018) Ryanodine Receptor-Mediated Calcium Release Has a Key Role in Hippocampal LTD Induction. *Front Cell Neurosci* 12:403. <https://doi.org/10.3389/fncel.2018.00403>
44. Zhang B, Wang L, Chen T, Hong J, Sha S, Wang J, Xiao H, Chen L (2017) Sigma-1 receptor deficiency reduces GABAergic inhibition in the basolateral amygdala leading to LTD impairment and depressive-like behaviors. *Neuropharmacology* 116:387–398. <https://doi.org/10.1016/j.neuropharm.2017.01.014>
45. Chidambaram SB, Rathipriya AG, Bolla SR, Bhat A, Ray B, Mahalakshmi AM, Manivasagam T, Thenmozhi AJ et al (2019) Dendritic spines: Revisiting the physiological role. *Prog Neuropsychopharmacol Biol Psychiatry* 92:161–193. <https://doi.org/10.1016/j.pnpbp.2019.01.005>
46. Lee KJ, Jung JG, Ariei T, Imoto K, Rhyu IJ (2007) Morphological changes in dendritic spines of Purkinje cells associated with motor learning. *Neurobiol Learn Mem* 88(4):445–450. <https://doi.org/10.1016/j.nlm.2007.06.001>
47. Arroyo ED, Fiole D, Mantri SS, Huang C, Portera-Cailliau C (2019) Dendritic Spines in Early Postnatal Fragile X Mice Are Insensitive to Novel Sensory Experience. *J Neurosci* 39(3):412–419. <https://doi.org/10.1523/jneurosci.1734-18.2018>
48. Padmashri R, Reiner BC, Suresh A, Spartz E, Dunaevsky A (2013) Altered structural and functional synaptic plasticity with motor skill learning in a mouse model of fragile X syndrome. *J Neurosci* 33(50):19715–19723. <https://doi.org/10.1523/jneurosci.2514-13.2013>

49. Abubakar A, Kipkemoi P (2022) Early intervention in autism spectrum disorder: The need for an international approach. *Dev Med Child Neurol* 64(9):1051–1058. <https://doi.org/10.1111/dmcn.15327>
50. Medishetti R, Rani R, Kavati S, Mahilkar A, Akella V, Saxena U, Kulkarni P, Sevilimedu A (2020) A DNzyme based knockdown model for Fragile-X syndrome in zebrafish reveals a critical window for therapeutic intervention. *J Pharmacol Toxicol Methods* 101:106656. <https://doi.org/10.1016/j.vascn.2019.106656>
51. Giacomini A, Stagni F, Emili M, Uguagliati B, Rimondini R, Bartesaghi R, Guidi S (2019) Timing of Treatment with the Flavonoid 7,8-DHF Critically Impacts on Its Effects on Learning and Memory in the Ts65Dn Mouse. *Antioxidants (Basel)* 8(6). <https://doi.org/10.3390/antiox8060163>
52. Seese RR, Le AA, Wang K, Cox CD, Lynch G, Gall CM (2020) A TrkB agonist and amphetamine rescue synaptic plasticity and multiple forms of memory in a mouse model of intellectual disability. *Neurobiol Dis* 134:104604. <https://doi.org/10.1016/j.nbd.2019.104604>
53. Uutela M, Lindholm J, Louhivuori V, Wei H, Louhivuori LM, Pertovaara A, Akerman K, Castrén E et al (2012) Reduction of BDNF expression in *Fmr1* knockout mice worsens cognitive deficits but improves hyperactivity and sensorimotor deficits. *Genes Brain Behav* 11(5):513–523. <https://doi.org/10.1111/j.1601-183X.2012.00784.x>
54. Darnell JC, Van Driesche SJ, Zhang C, Hung KY, Mele A, Fraser CE, Stone EF, Chen C et al (2011) FMRP stalls ribosomal translocation on mRNAs linked to synaptic function and autism. *Cell* 146(2):247–261. <https://doi.org/10.1016/j.cell.2011.06.013>
55. Chen ZY, Ieraci A, Teng H, Dall H, Meng CX, Herrera DG, Nykjaer A, Hempstead BL et al (2005) Sortilin controls intracellular sorting of brain-derived neurotrophic factor to the regulated secretory pathway. *J Neurosci: Off J Soc Neurosci* 25(26):6156–6166. <https://doi.org/10.1523/jneurosci.1017-05.2005>
56. Yoshii A, Constantine-Paton M (2010) Postsynaptic BDNF-TrkB signaling in synapse maturation, plasticity, and disease. *Dev Neurobiol* 70(5):304–322. <https://doi.org/10.1002/dneu.20765>
57. Emili M, Guidi S, Uguagliati B, Giacomini A, Bartesaghi R, Stagni F (2022) Treatment with the flavonoid 7,8-dihydroxyflavone: a promising strategy for a constellation of body and brain disorders. *Crit Rev Food Sci Nutr* 62(1):13–50. <https://doi.org/10.1080/10408398.2020.1810625>
58. Zeng Y, Liu Y, Wu M, Liu J, Hu Q (2012) Activation of TrkB by 7,8-dihydroxyflavone prevents fear memory defects and facilitates amygdalar synaptic plasticity in aging. *J Alzheimers Dis* 31(4):765–778. <https://doi.org/10.3233/jad-2012-120886>
59. Yang YJ, Li YK, Wang W, Wan JG, Yu B, Wang MZ, Hu B (2014) Small-molecule TrkB agonist 7,8-dihydroxyflavone reverses cognitive and synaptic plasticity deficits in a rat model of schizophrenia. *Pharmacol Biochem Behav* 122:30–36. <https://doi.org/10.1016/j.pbb.2014.03.013>

Publisher's Note Springer Nature remains neutral with regard to jurisdictional claims in published maps and institutional affiliations.

Springer Nature or its licensor (e.g. a society or other partner) holds exclusive rights to this article under a publishing agreement with the author(s) or other rightsholder(s); author self-archiving of the accepted manuscript version of this article is solely governed by the terms of such publishing agreement and applicable law.